AAPS PharmSciTech, Vol. 18, No. 4, May 2017 (© 2016)
DOI: 10.1208/s12249-016-0623-y

Research Article

Theme: Recent Trends in the Development of Chitosan-Based Drug Delivery Systems
Guest Editors: Claudio Salomon, Francisco Goycoolea, and Bruno Moerschbacher

Mucoadhesive Chitosan-Pectinate Nanoparticles for the Delivery of Curcumin to the Colon

Enas Alkhader,[1] Nashiru Billa,[1,3] and Clive J. Roberts[2]

Received 30 June 2016; accepted 23 August 2016; published online 31 August 2016

Abstract. In the present study, we report the properties of a mucoadhesive chitosan-pectinate nanoparticulate formulation able to retain its integrity in the milieu of the upper gastrointestinal tract and subsequently, mucoadhere and release curcumin in colon conditions. Using this system, we aimed to deliver curcumin to the colon for the possible management of colorectal cancer. The delivery system comprised of a chitosan-pectinate composite nanopolymeric with a z-average of 206.0 nm (±6.6 nm) and zeta potential of +32.8 mV (±0.5 mV) and encapsulation efficiency of 64%. The nanoparticles mucoadhesiveness was higher at alkaline pH compared to acidic pH. Furthermore, more than 80% release of curcumin was achieved in pectinase-enriched medium (pH 6.4) as opposed to negligible release in acidic and enzyme-restricted media at pH 6.8. SEM images of the nanoparticles after exposure to the various media indicate a retained matrix in acid media as opposed to a distorted/fragmented matrix in pectinase-enriched medium. The data strongly indicates that the system has the potential to be applied as a colon-targeted mucoadhesive curcumin delivery system for the possible treatment of colon cancer.

KEY WORDS: colon cancer; curcumin; mucoadhesive; nanoparticles; pectin.

INTRODUCTION

Despite recent research advances in cancer therapy, treatment options remains challenging and a significant number of cases are often referred to surgery, which is associated with high risk of damage to adjacent tissues, pain, infection and recurrence of the cancer (1–5). A less invasive option by way of radiation therapy manifests side effects such as skin changes, faecal incontinence, diarrhoea, nausea and vomiting which obviously affects quality of life (6–9). Further down the line in terms of non-invasiveness is chemotherapy which aptly is the first choice in the management of cancer. However, chemotherapy is also associated with side effects such as pain, sores in the mouth and throat, nausea and vomiting as well as blood disorders (10–15)

In order to mitigate some of the side effects due to chemotherapy, there is a growing interest in the use of anticancer agents of plant origin. These have been reported to manifest fewer side effects compared to their chemotherapeutic cousins (16–18).

Curcumin, commonly known as turmeric, is a natural polyphenol derived from the rhizome of the plant *Curcuma longa* and reported to have anticancer activity (19–24). Although curcumin has an effective and safe anticancer activity (25–27), its beneficial effects are limited due to poor absorption from the gastrointestinal tract along with rapid metabolism and clearance from the blood (28,29). For curcumin to present systematically as a favourable anticancer alternative, some form of formulation intervention is necessary. Using adjuvants like piperine, the oral bioavailability of curcumin was improved due to inhibition of curcumin metabolising enzymes by the former (30,31). The use of micelles, liposomes and phospholipid complexes has also been explored for the purpose of improving bioavailability of curcumin (32–35). More recently, nanoparticle formulation technology has gained traction as a viable alternative to the delivery of anticancer agents systematically (36,37). These nanoparticle delivery devices are often constructed from polymeric materials such as poly(lactide-co-glycolide) (PLGA), chitosan and poly-hydroxyethyl methacrylate/stearic acid (38–40).

In the present study however, our aim was not to improve the systemic bioavailability of curcumin, but rather to employ appropriate formulation strategies that ensure

[1] School of Pharmacy, Faculty of Science, University of Nottingham Malaysia Campus, Jalan Broga, 43500, Semenyih, Selangor Darul Ehsan, Malaysia.
[2] School of Pharmacy, University of Nottingham, University Park, Nottingham, NG7 2RD, UK.
[3] To whom correspondence should be addressed. (e-mail: Nashiru.Billa@nottingham.edu.my)

intact delivery of curcumin to the colon after oral administration, where curcumin may manifest its anticancer effects locally, through an added effect of mucoadhesion. In this regard, the delivery system must retain its integrity and protect curcumin from the variable hydrodynamics and milieu of the upper gastrointestinal tract as it transits from the mouth to the colon. The latter is reinforced because of the instability of curcumin in acidic media. Such a delivery system is likely to materialise with enhanced therapy due to the restriction of the disease to the colon and a possible high payload dumping of curcumin at the colon due to localised enzymatic effect on the formulation. In a previous study, we reported that chitosan-curcumin nanoparticles demonstrated mucoadhesive and anticancer properties (41). In this study, the formulation has been modified to address the buffering potential in acidic conditions, whilst manifesting enhanced mucoadhesion in colonic conditions.

Chitosan is used here because it is biodegradable and used extensively as a pharmaceutical excipient (42–46). Recently, it has been investigated for use in novel drug delivery applications such as carriers for vaccines and DNA (47,48). When suitably formulated, it also possesses mucoadhesive properties.

Pectin is an anionic and soluble polysaccharide extracted from the primary cell walls of plants. It is widely and safely used in food and pharmaceutical industries (49,50). Pectin passes intact through the upper gastrointestinal tract and is degraded by colonic microflora (51,52). Furthermore, pectin is mucoadhesive at alkaline pH of the colon (53). However, when used alone, pectin swells at alkaline conditions which may lead to premature release of drug payload. When used in conjunction with other polymers however, more stable matrices are formed (54). Therefore, pectin was used along with chitosan in the formulation of the nanoparticles in order to restrict premature release of curcumin at lower pH but to ensure enhanced mucoadhesive properties at the colonic condition. Furthermore, pectin is susceptible to colonic microbial degradation, which would ensure release of curcumin from the composite polymer matrices locally.

MATERIALS AND METHODS

Curcumin analytical standard was purchased from Fluka, USA. Low molecular weight chitosan and sodium tripolyphosphate (TPP) was purchased from Sigma Aldrich, USA. Low methoxy pectin was from CP Kelco, USA, and mucin type III from porcine stomach was purchased from Sigma-Aldrich, USA. Pectinase (*Aspergillus niger*) was purchased from Abnova, Taiwan. Glacial acetic acid and absolute ethanol were purchased from R&M Chemicals, UK. Acetonitrile (HPLC grade) was purchased from RCI Labscan, Thailand.

Formulations of Curcumin Chitosan-Pectinate Nanoparticles

A 300 μl aliquot solution of curcumin in ethanol (1 mg/ml) was added dropwise to 25 ml of pectin solution (0.05 g/ml) and then 25 ml of (0.15 g/ml) chitosan solution in 2% *v/v* acetic acid with different concentrations, which pH was adjusted to 5 using 2 M NaOH. The mixture was stirred at 500 rpm for 60 min on a magnetic stirrer followed by addition of 25 ml of (0.05 g/ml) TPP and further stirring at 500 rpm for 60 min.

Further optimisation was carried out by varying the quantities of chitosan, TPP and pectin (3:1:1, 3:2:1, 4:1:1, 4:2:1, 5:1:1 and 5:2:1, respectively), stirring speed (500, 800 and 1000 rpm) and stirring time (2 min/20 min, 2 min/40 min, 2 min/60 min), upon the addition of chitosan and TPP, respectively.

Size and Zeta Potential Measurement

The z-average diameter and zeta potentials of freshly prepared CS-PEC-NPs and CUR-CS-PEC-NPs and those exposed to acidic (pH 1.2) and alkaline (pH 6.8) media were determined using a Zeta Sizer Nano Series® (Malvern Instruments, UK) equipped with a 4-mW He-Ne laser at wavelength of 633 nm. Hydrodynamic diameter (*d*, nm) was measured by dynamic laser scattering (DLS) at a scattering angle of 173°. The CS-PEC-NPs and CUR-CS-PEC-NPs were diluted 5- and 10-fold, respectively, with deionised water prior to measurements. Samples were run in triplicate and mean reading was taken.

Morphological and Surface Topography

The morphology and surface topography of the CUR-CS-PEC-NPs were observed using field emission scanning electron microscopy (FESEM) (Model Quanta 400F, FEI Company, USA) at an accelerating voltage of 5 kV. Samples were prepared by placing one drop of NPs suspension on the stub and left to dry at ambient temperature 24 h before viewing. Nanoparticles exposed to acidic (pH 1.2), alkaline (pH 7.4) and alkaline (pH 6.4) with pectinase were observed for morphological changes using the FESEM described above.

Fourier Transform Infrared (FTIR) Analysis and X-Ray Diffractometry

Evidence of chemical association within the nanoparticles was ascertained using a Spectrum RX1 FTIR spectrometer (Perkin Elmer, USA) and an XRD 7000 diffractometer (Shimadzu, Japan). Samples for the FTIR analysis were prepared using potassium bromide (KBr) at 98:2 *w/w* ratio of KBr to freeze-dried nanoparticles, respectively, and then compressed into a 5-mm disc using a Carver pressor®, Carver Inc. USA at 5 ton pressure for 5 min. FTIR scans were acquired between 4000 and 400 cm^{-1} with 64 runs at a resolution of 4 cm^{-1} using an interval of 1 cm^{-1}. For the XRD analysis, freeze-dried samples were finely grounded and prepared as a film followed by irradiation with CuKα generated at 40 kV and 80 mA. Data were recorded at 2θ range between 0 and 40°C at a scanning speed of 0.5°/min using Maxima XRD7000, Shimadzu, Japan.

Differential Scanning Calorimetry (DSC)

Thermal analysis on formulations was carried out using Q2000 (TA Instruments, USA) differential scanning calorimeter under a gentle stream (20 ml/min) of nitrogen gas. Sample weight ranged from 8 to 12 mg except for curcumin

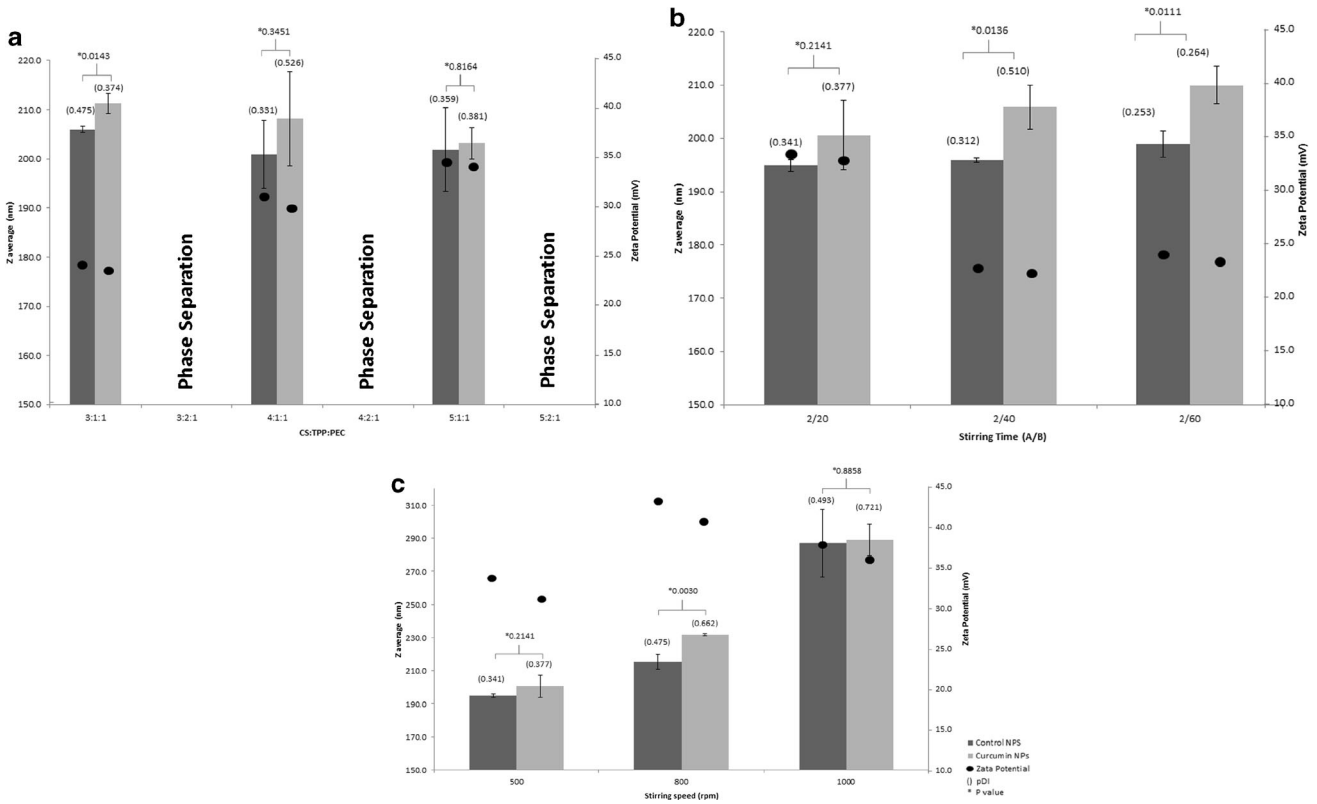

Fig. 1. Z-average, zeta potential and pDI of CS-PEC-NPs and CUR-CS-PEC-NPs as a function of formulation ratios (**a**), stirring time (**b**) and stirring speed (**c**)

which was 3 mg. Samples were prepared in aluminium pans using a standard pneumatic press and then heated from 0 to 320°C at rate of 5°C/min. The reference was sealed aluminium pan.

Determination of Encapsulation Efficiency

The unbound curcumin in the supernatant and the weakly adsorbed curcumin on the surface of the CUR-CS-PEC-NPs were collected by centrifugation and washed off twice with methanol, respectively. The amount of curcumin in the methanol rinse and the supernatant were both analysed to determine the total unbound curcumin by injecting 20 µl onto an HPLC system (55). Briefly, the mobile phase comprised of 2% acetic acid (*v*/*v*)/acetonitrile (60:40) run at 2 ml/min and response detected at a wavelength of 425 nm. The amount of curcumin in the samples was obtained by comparing peak area obtained with those from a standard curve treated similarly. The percentage of encapsulated curcumin was calculated as follows:

$$\%\text{Encapsulation Efficiency} = \frac{\text{Total curcumin added} - \text{unbound curcumin}}{\text{Total curcumin added}} \times 100\%$$

The encapsulation capacity was calculated as follows

$$\%\ \text{Encapsulation Capacity} = \frac{\text{Weight of encapsulated curcumin (mg)}}{\text{Weight of nanoparticles (mg)}} \times 100\%$$

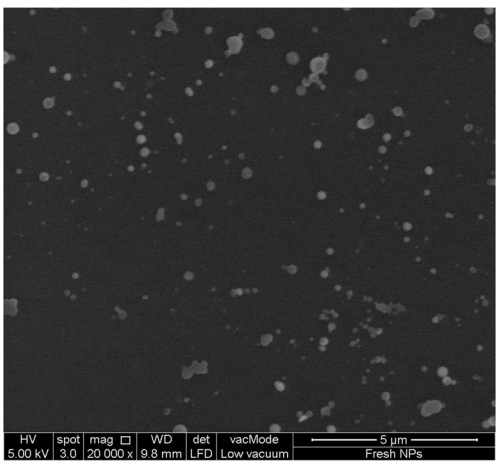

Fig. 2. SEM image of the optimised formulation

Curcumin Release from Nanoparticles

CUR-CS-PEC-NPs collected by centrifugation was washed and suspended in phosphate buffer saline (pH 6.4) containing 1% (*w*/*v*) Tween 80 and 2.5% (*w*/*v*) pectinase enzyme to a final concentration of 10 mg CUR-CS-PEC-NPs per ml of solution. Similarly, the CUR-CS-PEC-NPs were

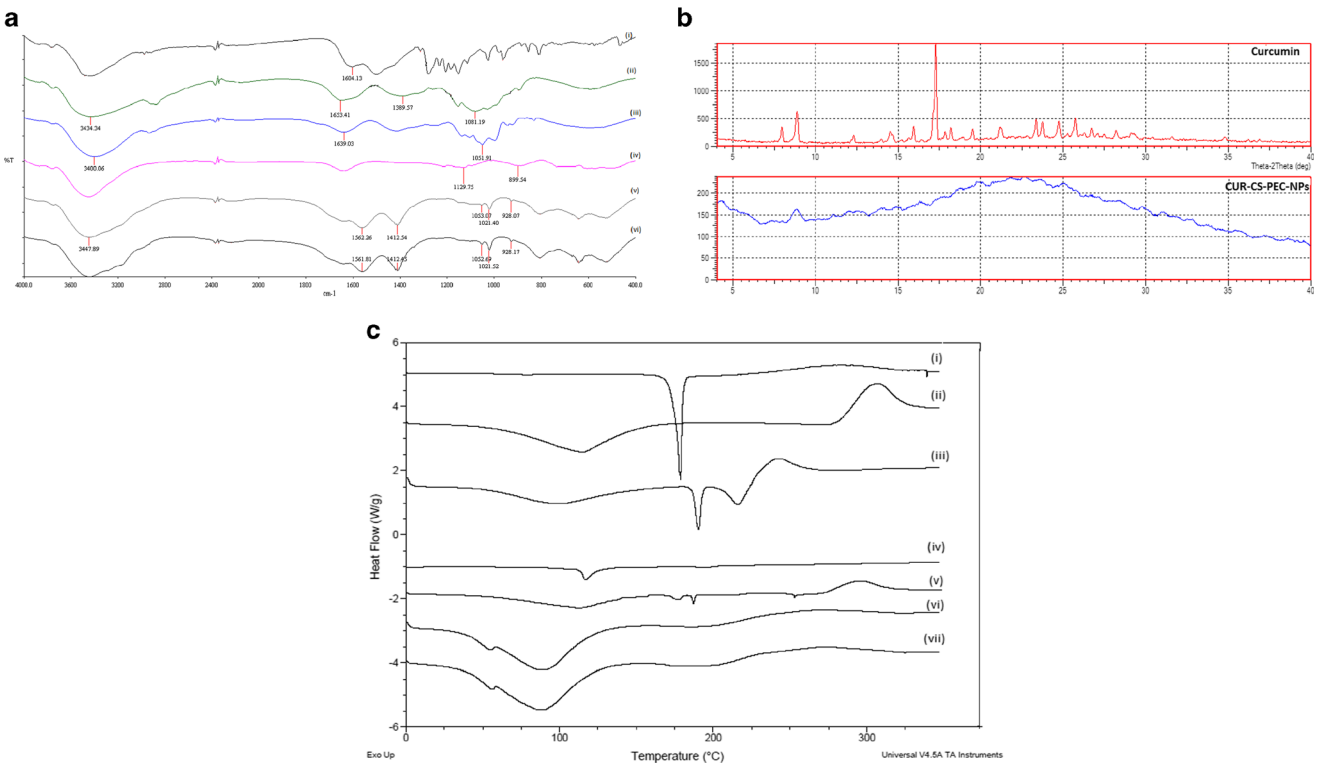

Fig. 3. **a** FTIR spectra of curcumin (*i*), chitosan (*ii*), pectin (*iii*), TPP (*iv*), CS-PEC-NPs (*v*) and CUR-CS-PEC-NPs (*vi*). **b** XRD patterns of curcumin and CUR-CS-PEC-NPs. **c** DSC thermograms of curcumin (*i*), chitosan (*ii*), pectin (*iii*), TPP (*iv*), physical mixture of pectin and curcumin (*v*), CS-PEC-NPs (*vi*) and CUR-CS-PEC-NPs (*vii*)

suspended in 0.1 N HCl (pH 1.2) and HEPES buffer (pH 6.8). Each of the three types of dissolution media containing CUR-CS-PEC-NPs were seeded into eight sampling vials and subjected to rotary shaking at 180 rpm (WiseCube®, Witeg Inc., Germany) incubated at 37°C. Curcumin release was studied over 6 h at 20 min, 40 min, 1 h, 2 h, 3 h, 4 h, 5 h and 6 h by withdrawing one vial and its content centrifuged at 4000 rpm for 10 min to pellet the particles. The amount of curcumin released was determined in the supernatant using the HPLC method described above in three independent runs and reported as the mean of these runs.

Since the CUR-CS-PEC-NPs are designed to transit the upper GIT followed by the alkaline conditions of the distal GIT, the effect that this variable pH might have on the physical integrity of the CUR-CS-PEC-NPs was studied by suspending the nanoparticles in pH 1.2 for 1 h, retrieving by centrifugation and then exposing them in pH 6.8 for 2 h. The zeta potential values and percentage retention of curcumin were determined as described above.

Mucoadhesion Studies

The mucoadhesive propensities of the CUR-CS-PEC-NPs were determined by dispersing them in type III mucin solution from porcine stomach at 0.1, 0.2, 0.4 and 0.6 mg/ml. The magnitude of mucoadhesion was obtained by measuring the changes in the zeta potential of the particles after interaction with mucin (56,57). The CUR-CS-PEC-NPs mucin suspension was vortex mixed for 1 min followed by incubation in an incubating shaker operated at 180 rpm for 1 h at 37°C. The zeta potential of the nanoparticles was then measured using the Zetasizer and the drop in zeta potential recorded as a measure of degree of interaction of CUR-CS-PEC-NPs with mucin.

RESULTS AND DISCUSSION

The size, pDI and zeta potential of the CS-PEC-NPs were 206.0 ± 0.6 nm, 0.475 and 24.0 ± 0.3 mV, respectively, whilst those for CUR-CS-PEC-NPs were 211.3 ± 2.0 nm, 0.374 and 23.5 ± 0.4 mV. Thus, there was an increase in the size of the particles after incorporation of curcumin; however, this increase was statistically significant ($p = 0.0143$). The formation of the nanoparticles is based on electrostatic interaction between the deprotonated negative charge of the carboxylic acid moiety of pectin ($-COO^-$) interacting with the protonated positively charged amine ($-NH_3^+$) groups of chitosan. The addition of TPP results in crosslinking network between the triphosphate moiety ($-P_3O_{10}^-$) of TPP and $-NH_3^+$ of chitosan. The crosslinking allows primary interactions between pectin and chitosan to be further pulled inward so that the particles assume a spherical shape and become smaller. The zeta potential for both CS-PEC-NPs and CUR-CS-PEC-NPs was positive and this can be attributed to the residual $-NH_3^+$ in chitosan. Curcumin is known to exist in tautomeric forms such as the 1,3,-diketo and two equivalent enols forms (58). The enol form ($-RCO_4^-$) predominates in organic solvents as in the present study and competes with the TPP ($-P_3O_{10}^-$) for $-NH_3^+$ groups of chitosan. Additionally, the presence of curcumin impedes

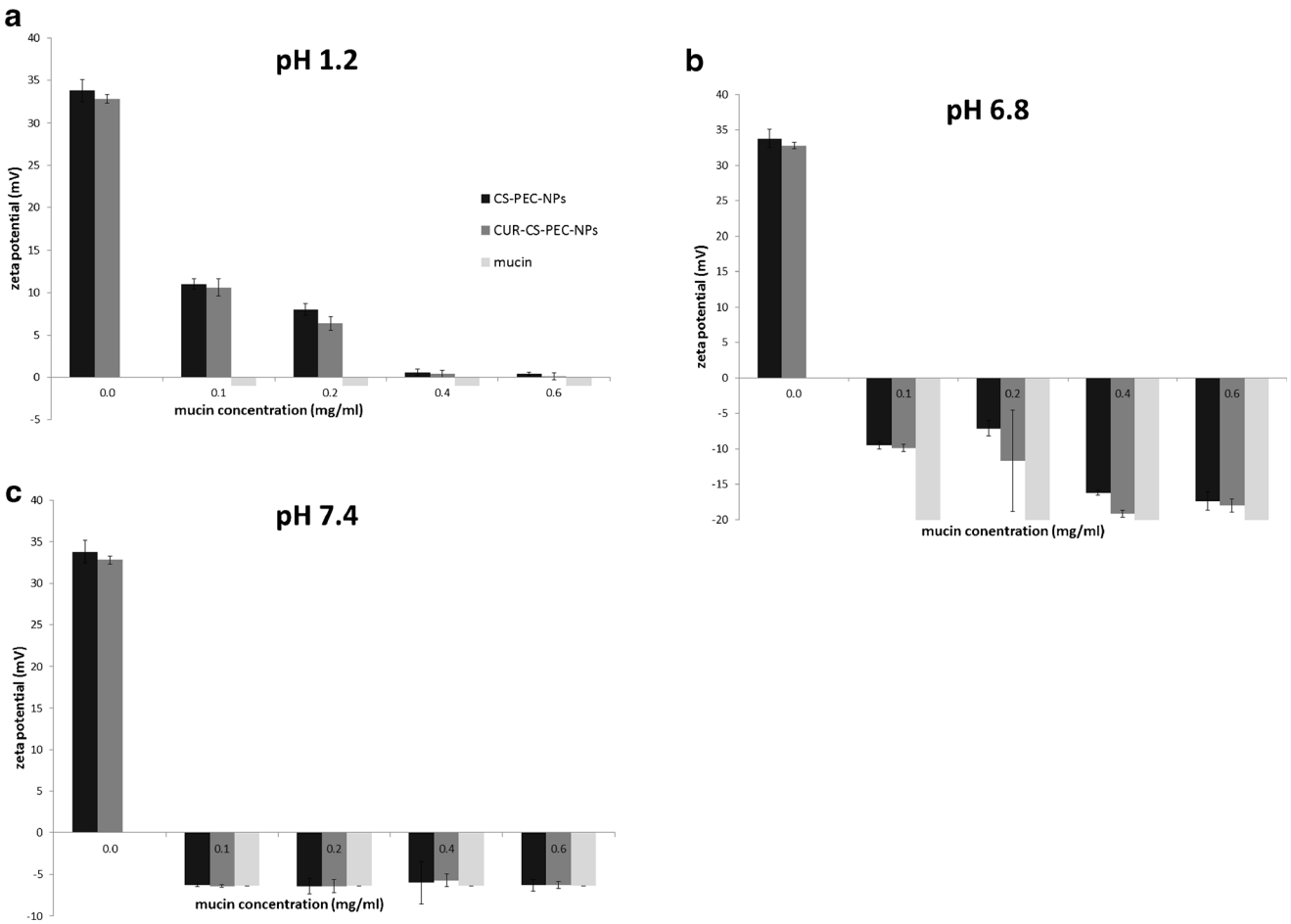

Fig. 4. Changes in zeta potential of CUR-CS-PEC-NPs and CS-PEC-NPs in pH 1.2 (**a**), pH 6.8 (**b**) and pH 7.4 (**c**)

reproach by TPP toward free $-NH_3^+$ due to stearic hindrance by the former so that the z-potential of CUR-CS-PEC-NPs was lower relative to CS-PEC-NPs. The encapsulation efficiency was 64%, which suggest that the CUR-CS-PEC-NPs retained a significant load although the loading capacity was 0.096%.

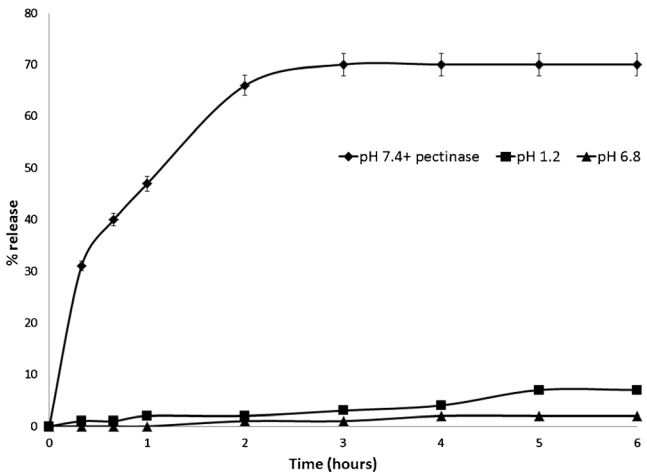

Fig. 5. Curcumin release from CUR-CS-PEC-NPs in pH 1.2, 6.8 and 6.4 (plus pectinase)

Effect of Formulation Variables on Physical Properties of Nanoparticles

In order to study the effects of formulation variables on the physical properties of the nanoparticles, a series of formulas were studied by varying the ratio of CS/TPP/PEC. Figure 1a shows that an increase in the TPP ratio caused a dramatic increase in the size of the particles, causing phase separation. This could be due to increased inter- and intramolecular interactions between TPP and chitosan and pectin. On the other hand, increase in chitosan concentration caused a decrease in the size of the nanoparticles and this is attributable to the heightened level of interaction between free amino group ($-NH_3^+$) of chitosan with the negative phosphate ($-P_3O_{10}^-$) and carboxylic (COO^-) groups in TPP and pectin, respectively. Particles with lowest z-average were obtained at 5:1:1. In terms of applicability to the current pursuit, nanoparticles with low z-average are desirable due to high surface-to-volume ratio. Subsequently, this ratio was selected for studying effect of stirring time and stirring speed on the physical properties of the nanoparticles.

From the data in Fig. 1b, we observed a direct relation between the stirring time and the z-average for both CUR-CS-PEC-NPs and CS-PEC-NPs. This could be explained by the fact that as the nanoparticles are formed initially,

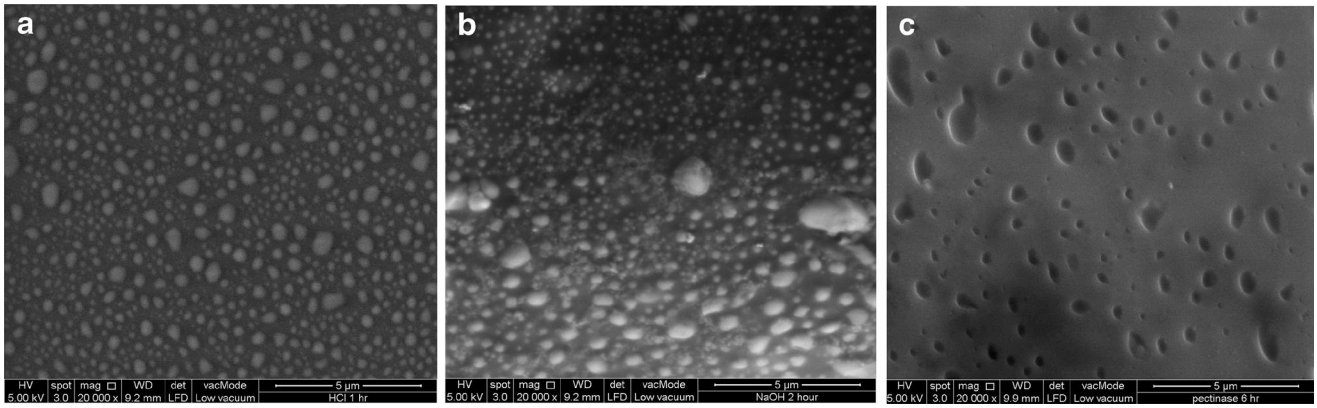

Fig. 6. SEM image of CUR-CS-PEC-NPs in acidic medium (**a**), 2 h in alkaline medium (**b**), 6 h alkaline medium plus pectinase (**c**)

further stirring of the component results in disrupting the ionic gel of the previously formed particles. This disruption of the nanoparticle fabric also causes a decrease in zeta potential with longer stirring time. From a formulation and stability standpoint, a stirring speed of 500 rpm for 2 min after the addition of chitosan to pectin followed by an additional 20 min of stirring after the addition of TPP was deemed applicable. The formulation was further optimised using stirring speeds of 500, 800 and 1000 rpm and the data on the effect of stirring speed on the physical properties of both the CUR-CS-PEC-NPs and CS-PEC-NPs are presented in Fig. 1c. Stirring speed of 500 rpm not only produced the desired lower z-average, but also a lower pDI and high zeta potential. This effect of stirring speed on size of the nanoparticles has also been reported previously (59,60) and is attributed to high shear forces disrupting the crosslinked fabric of the nanoparticles imposed by TPP much, like the effects of extended stirring times described earlier.

Morphology of CUR-CS-PEC-NPs

Figure 2 shows the FESEM image of the CUR-CS-PEC-NPs of the optimised formulation, which appear spherical and the sizes are in agreement with those obtained from the photon correlation analysis described above. The particles also appear to be well separated from each other which suggest that sufficient electrical charge is retained by the dispersion. The surface of the nanoparticles is free of cracks or fissures which indicate effective crosslinking.

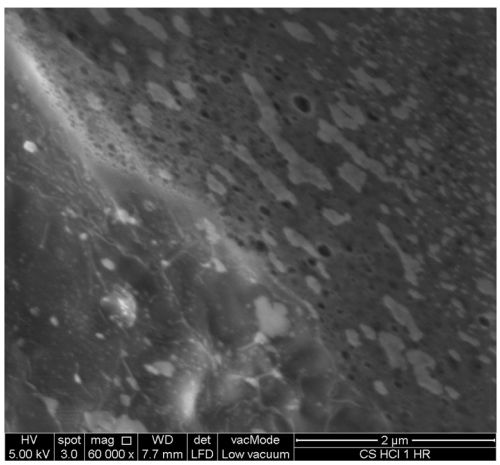

Fig. 7. SEM image of pectin-free nanoparticles in acidic medium

FTIR and X-Ray Diffractometry

The FTIR spectra of the raw materials and formulated nanoparticles are presented in Fig. 3a. In the raw materials, stretching vibrations of C=O group of curcumin (i) appears at 1604 cm^{-1}. No peaks can be observed within the range of 1800–1650 cm^{-1} which suggests that curcumin is present in the keto-enol tautomeric form (61). The chitosan spectrum (ii) shows a broad peak at 3434 cm^{-1} which is attributed to the stretching vibration of the hydroxyl groups whilst the amide I stretching of the carbonyl groups presents at 1653 cm^{-1}. Furthermore, a peak appears at 1389 cm^{-1} corresponds to the N-H stretching of amide and ether bonds and the peak at 1081 cm^{-1} assigns to a secondary hydroxyl group (62,63). The broad peak of pectin (iii) at 3400 cm^{-1} is assigned to the stretching frequency of -OH group. The peak at 1051 cm^{-1} is related to C=C or C=O double bonds within pectin while the peak at 1639 cm^{-1} is assigned to asymmetric stretching bands of COO^{-} groups (64,65). The characteristic peak at 1129 cm^{-1} is assigned to P=O groups of TPP (iv) while the one at 899 cm^{-1} is related to the P-O-P asymmetric stretching (66,67). These bands were all present in both the formulations CUR-CS-PEC-NPs and CS-PEC-NPs, spectra (v and vi, respectively). We may conclude that these groups are not typically involved in covalent chemical bonding with the other components during the formulation process. The CUR-CS-PEC-NPs FTIR spectrum is similar to the CS-PEC-NPs spectrum except for a slight shifting of the amine peak at 1562 cm^{-1} which is attributed to curcumin loading in CUR-CS-PEC-NPs (63). Furthermore, the peak attributed to curcumin is absent in the CUR-CS-PEC-NPs spectrum which assures curcumin loading in the latter. The XRD data of curcumin (Fig. 3b) shows multiple peaks at 2θ range of 7–30° intimating its crystalline state. However, these peaks are absent in CUR-CS-PEC-NPs suggesting that the curcumin is present in the amorphous state. This is crucially significant because an amorphous arrangement ensures a rapid rate of release.

Table I. Zeta Potential and Percentage Retention of Curcumin in CUR-CS-PEC-NPs After Exposure to pH 1.2 and 6.8

	Fresh CUR-CS-PEC-NPs	pH 1.2	pH 6.8
Zeta potential (mV)	+33.1 ± 1.1	+37.9 ± 2.5	+33 ± 1.3
Retention (%)	64% ± 2%	62% ± 2%	60% ± 1%

DSC Analyses

In order to further ascertain the physical nature of the nanoparticles, thermal analyses were carried out on both the optimised CUR-CS-PEC-NPs and CS-PEC-NPs in comparison with the raw materials. Figure 3c shows the DSC data where curcumin (i) shows a sharp melting peak at 178.7°C whilst chitosan (ii) shows endothermal peak at 113.9°C and an exothermic peak at 307.4°C. Pectin (iii) has a transition peak at 190°C. Endothermic peaks are correlated with loss of water associated with the hydrophilic groups of chitosan while the exothermic peaks result from the degradation of polyelectrolytes followed by the hydration and depolymerization reactions which happen due to the partial decarboxylation of the protonated carboxylic groups and oxidation reactions of the polyelectrolytes (68). TPP (iv) shows melting point of the salt at 116.6°C. The thermograms of the physical mixture of chitosan, TPP, pectin and curcumin (v) showed similar peaks observed in the pure samples. Thermograms of the formulations (CS-PEC-NPs and CUR-CS-PEC-NPs), (vi) and (vii), respectively, showed a broad endothermic peak at about 89.5°C, which appear to be a shift of the TPP peak at 112°C (iv). This broadening of the peak in the formulations is due to complexation of TPP because the sharpness of this peak in the physical mixture is lost but prominent in TPP. There is a broad exothermic peak at 269.3°C in both formulations and this is due to chitosan but is slightly shifted from the peak at 307.4°C in pure chitosan because of weak interaction. Furthermore, the melting point of curcumin cannot be seen in the thermograms of CUR-CS-PEC-NPs because curcumin is molecularly dispersed in the NPs in the amorphous state. Thus, the data from the DSC analysis complement those of the FTIR and X-ray diffractometry.

Mucoadhesive Properties of the Optimised Formulation

The mucoadhesive properties of the optimised CS-PEC-NPs and CUR-CS-PEC-NPs formulation were studied at four concentrations of mucin maintained in pH 1.2, 6.8 and 7.4. There was a direct relationship between the drop in zeta potential and mucin concentration as presented in Fig. 4a. The drop in zeta potential is a measure of the extent of mucoadhesion of the nanoparticles by mucin (56). Consequently, the drop in zeta potential of the CUR-CS-PEC-NPs and CS-PEC-NPs at pH 6.8 was more drastic compared to in pH 1.2 (Fig. 4b), suggesting that the nanoparticles are more mucoadhesive at pH 6.8. At pH 7.4 (Fig. 4c), both CS-PEC-NPs and CUR-CS-PEC-NPs have higher mucoadhesion than in both pH 1.2 and 6.8; however, the extent of adhesion is similar for CUR-CS-PEC-NPs compared to CS-PEC-NPs. Variation in pH affects the surface charge on mucin, CS-PEC-NPs and CUR-CS-PEC-NPs. Mucin has sialic acid residues which have a pKa of 2.6, resulting in a negative charge at physiological pH (pH 7.4). There was a positive correlation between the drop in zeta potential and pH and this can be explained by the fact that at higher pH the ionised carboxyl functional groups of mucin (COO^-) repel each other and change the spatial conformation from a coiled state into a "rod-like" structure, which results in making them more accessible for inter-diffusion and interpenetration (69). The COO^- in mucin allows the positively charged $-NH_4^+$ groups of chitosan to form polyelectrolyte complexes which results in mucoadhesion. At higher pH, the amine groups in chitosan become more positive and therefore forms stronger polyelectrolyte bonds with mucin. Therefore the particles are completely covered by mucin at higher pH and thus register identical zeta potential as mucin.

Curcumin Release from CUR-CS-PEC-NPs

Curcumin release in pH 1.2, 6.8 and 6.4 (in the presence of pectinase) are presented in Fig. 5. Besides this, CUR-CS-PEC-NPs morphology was studied at the same pH variations used in the release studies. Since chitosan and pectin have different pKa values (6.1–6.5 and 2.9–4.1, respectively), they act differently in terms of protonation/deprotonation as a function of pH. In acidic conditions (pH 1.2), both the amine groups of chitosan and the carboxylic groups of pectin are protonated. Since the ionisation of carboxylic groups of pectin is limited, and it has the dominant effect, the coulombic repulsion of the carboxylic groups is reduced which protects the NPs. However, a slight swelling (Fig. 6a) and negligible leaching of curcumin were observed at this pH. At pH 6.8, the carboxylic groups of pectin become deprotonated and hence electrostatic repulsion between ionised groups lead to chain repulsion. However, the amine group of chitosan is protonated and more electrostatic interaction between $-NH_3^+$ and $-COO^-$ is formed so that nanoparticles' swelling is impeded (Fig. 6b). Despite this interaction and crosslinking, pectinase randomly catalysing the cleavage of α-1,4-glycosidic linkages of pectin breaks existing bond formation between pectin and chitosan causing a burst release of 15% of curcumin obtained in the first 20 min (70). A plateau was manifested in 5 h with more than 80% at end of study. Figure 6c shows the morphology of CUR-CS-PEC-NPs after 6 h treatment in pectinase enzyme at pH 6.4. The nanoparticles appear dark which might be due to the enzymatic digestion (71–73). Pectinase is one of several enzymes produced by colonic bacteria and shows here that the above formulation is not only mucoadhesive at alkaline conditions but

also releases curcumin significantly in the presence of colonic enzyme. In order to study the protective effects of pectin against the acidic media of the upper GIT, pectin-free NPs were suspended in a 0.1 N HCl solution (pH 1.2) for 1 h and the morphology of the NPs was studied under FESEM (Fig. 7). The NPs appear deformed and distorted after this treatment, which suggests degradation of the particles.

From Table I we note that there was an increase in the zeta potential of the nanoparticles after exposure to pH 1.2, representing the stomach. This increase in zeta potential is due to protonation of the amine groups of chitosan. At this pH, there is also a reduction in the magnitude of the negative charge on the carboxylic moiety of pectin due to protonation. This combined effect on the amine groups and carboxylic acid in acidic media contributes to rise in surface charge. On the other hand, exposure of the CUR-CS-PEC-NPs to pH 6.4 (representing the colon pH) after treatment in pH 1.2 caused a fall in the zeta potential to the initial value. This change in zeta potential can be attributed to the deprotonation of the carboxylic group of pectin to the charged species ($-COO^-$), allowing electrostatic interaction between $-NH_3^+$ of chitosan. In parallel, the percentage retention of curcumin within the CUR-CS-PEC-NPs was ascertained after exposure to the different media. The percentage retention of curcumin decreased slightly after exposure to pH 1.2, with further decrease in pH 6.4; however, this decrease is minimal and suggests that the CUR-CS-PEC-NPs have the potential to retain a significant amount of the payload against variable pH profile.

CONCLUSION

A curcumin-containing chitosan-pectinate composite nanoformulation was successfully formulated and optimised. Mucoadhesion is strongest in alkaline conditions and dependent on mucin concentration. Crucially, the nanoparticles retained a significant curcumin payload after exposure in acidic and then alkaline media. We may conclude that the above formulation has the potential for possible delivery to the colon for localised curcumin activity whereby, through a combination of mucoadhesion and enzymatic degradation on the matrix, the therapeutic effect may manifest effectively.

COMPLIANCE WITH ETHICAL STANDARDS

Conflict of Interest The authors report no conflicts of interest.

REFERENCES

1. Bornstein BA, Recht A, Connolly JL, Schnitt SJ, Cady B, Koufman C, *et al*. Results of treating ductal carcinoma in situ of the breast with conservative surgery and radiation therapy. Cancer. 1991;67:7–13. doi:10.1002/1097-0142%2819910101%2967%3A1%3C7%3A%3AAID-CNCR2820670103%3E3.0.CO%3B2-B.
2. Cohen L, Hack TF, Moor C De, Katz J, Goss PE. The effects of type of surgery and time on psychological adjustment in women after breast cancer treatment. Ann Surg Oncol. 2000;7:427–34.
3. Takahashi H, Okabayashi K, Tsuruta M, Hasegawa H, Yahagi M, Kitagawa Y. Self-expanding metallic stents versus surgical intervention as palliative therapy for obstructive colorectal cancer: a meta-analysis. World J Surg. 2015;39:2037–44.
4. Schiphorst AH, Verweij NM, Pronk A, Borel Rinkes IH, Hamaker ME. Non-surgical complications after laparoscopic and open surgery for colorectal cancer—a systematic review of randomised controlled trials. Eur J Surg Oncol. 2015;41:1–10.
5. Haanstra JF, de Vos Tot Nederveen Cappel WH, Gopie JP, Vecht J, Vanhoutvin SA, Cats A *et al*. Quality of life after surgery for colon cancer in patients with Lynch syndrome: partial versus subtotal colectomy. Dis Colon Rectum. 2012;55:653–9.
6. Bourgier C, Levy A, Vozenin MC, Deutsch E. Pharmacological strategies to spare normal tissues from radiation damage: useless or overlooked therapeutics? Cancer Metastasis Rev. 2012;3:699–712.
7. Sia J, Joon DL, Viotto A, Mantle C, Quong G, Rolfo A, *et al*. Toxicity and long-term outcomes of dose-escalated intensity modulated radiation therapy to 74 Gy for localised prostate cancer in a single Australian centre. Cancers. 2011;3:3419–31.
8. Van Gijn W, Marijnen CAM, Nagtegaal ID, Kranenbarg EMK, Putter H, Wiggers T, *et al*. Preoperative radiotherapy combined with total mesorectal excision for resectable rectal cancer: 12-year follow-up of the multicentre, randomised controlled TME trial. Lancet Oncol. 2011;12:575–82. doi:10.1016/S1470-2045(11)70097-3.
9. Bruheim K, Guren MG, Skovlund E, Hjermstad MJ, Dahl O, Frykholm G, *et al*. Late side effects and quality of life after radiotherapy for rectal cancer. Int J Radiat Oncol Biol Phys. 2010;76:1005–11.
10. Farrell C, Brearley SG, Pilling M, Molassiotis A. The impact of chemotherapy-related nausea on patients' nutritional status, psychological distress and quality of life. Support Care Cancer. 2013;21:59–66.
11. Henry DH, Langer CJ, McKenzie RS, Piech CT, Senbetta M, Schulman KL, *et al*. Hematologic outcomes and blood utilization in cancer patients with chemotherapy-induced anemia (CIA) pre- and post-national coverage determination (NCD): results from a multicenter chart review. Support Care Cancer. 2012;20:2089–96.
12. Grothey A, Nikcevich DA, Sloan JA, Kugler JW, Silberstein PT, Dentchev T, *et al*. Intravenous calcium and magnesium for oxaliplatin-induced sensory neurotoxicity in adjuvant colon cancer: NCCTG N04C7. J Clin Oncol. 2011;29:421–7.
13. Sonis S, Treister N, Chawla S, Demetri G, Haluska F. Preliminary characterization of oral lesions associated with inhibitors of mammalian target of rapamycin in cancer patients. Cancer. 2010;116:210–5.
14. Peterson DE, Bensadoun RJ, Roila F. Management of oral and gastrointestinal mucositis: ESMO clinical practice guidelines. Ann Oncol. 2011;22:78–84.
15. Qi F, Li A, Inagaki Y, Gao J, Li J, Kokudo N, *et al*. Chinese herbal medicines as adjuvant treatment during chemo- or radiotherapy for cancer. Biosci Trends. 2010;4:297–307.
16. Faried A, Kurnia D, Faried LS, Usman N, Miyazaki T, Kato H, *et al*. Anticancer effects of gallic acid isolated from Indonesian herbal medicine, *Phaleria macrocarpa* (Scheff.) Boerl, on human cancer cell lines. Int J Oncol. 2007;30:605–13.
17. Nirmala MJ, Samundeeswari A, Sankar PD. Natural plant resources in anti-cancer therapy—a review. Res Plant Biol. 2011;1:1–14.
18. Pezzuto JM. Plant-derived anticancer agents. Biochem Pharmacol. 1997;53:121–33.
19. Adams BK, Ferstl EM, Davis MC, Herold M, Kurtkaya S, Camalier RF, *et al*. Synthesis and biological evaluation of novel curcumin analogs as anti-cancer and anti-angiogenesis agents. Bioorg Med Chem. 2004;12:3871–83.
20. Duvoix A, Blasius R, Delhalle S, Schnekenburger M, Morceau F, Henry E, *et al*. Chemopreventive and therapeutic effects of curcumin. Cancer Lett. 2005;223:181–90.
21. Sa G, Das T. Anti cancer effects of curcumin: cycle of life and death. Cell Div. 2008;3:14.

22. Kanai M, Imaizumi A, Otsuka Y, Sasaki H, Hashiguchi M, Tsujiko K, *et al*. Dose-escalation and pharmacokinetic study of nanoparticle curcumin, a potential anticancer agent with improved bioavailability, in healthy human volunteers. Cancer Chemother Pharmacol. 2012;69:65–70.
23. Li M, Zhang Z, Hill DL, Wang H, Zhang R. Curcumin, a dietary component, has anticancer, chemosensitization, and radiosensitization effects by down-regulating the MDM2 oncogene through the PI3K/mTOR/ETS2 pathway. Cancer Res. 2007;67:1988–96.
24. Lee J-W, Park S, Kim SY, Um SH, Moon E-Y. Curcumin hampers the antitumor effect of vinblastine via the inhibition of microtubule dynamics and mitochondrial membrane potential in HeLa cervical cancer cells. Phytomedicine [Internet]. Elsevier GmbH. 2016;23:705–13.
25. Tang H, Murphy CJ, Zhang B, Shen Y, Van Kirk EA, Murdoch WJ, *et al*. Curcumin polymers as anticancer conjugates. Biomaterials. 2010;31:7139–49. doi:10.1016/j.biomaterials.2010.06.007.
26. Howells LM, Sale S, Sriramareddy SN, Irving GRB, Jones DJL, Ottley CJ, *et al*. Curcumin ameliorates oxaliplatin-induced chemoresistance in HCT116 colorectal cancer cells in vitro and in vivo. Int J Cancer. 2011;129:476–86.
27. Babaei E, Sadeghizadeh M, Hassan ZM, Feizi MAH, Najafi F, Hashemi SM. Dendrosomal curcumin significantly suppresses cancer cell proliferation in vitro and in vivo. Int Immunopharmacol. 2012;12:226–34.
28. Li L, Ahmed B, Mehta K, Kurzrock R. Liposomal curcumin with and without oxaliplatin: effects on cell growth, apoptosis, and angiogenesis in colorectal cancer. Mol Cancer Ther. 2007;6:1276–82.
29. Anand P, Kunnumakkara AB, Newman RA, Aggarwal BB, Anand P, Kunnumakkara AB, et al. Bioavailability of curcumin : problems and promises. Mol Pharma. 2007;4:807–18.
30. Bhutani MK, Bishnoi M, Kulkarni SK. Anti-depressant like effect of curcumin and its combination with piperine in unpredictable chronic stress-induced behavioral, biochemical and neurochemical changes. Pharmacol Biochem Behav. 2009;92:39–43. doi:10.1016/j.pbb.2008.10.007.
31. Sehgal A, Kumar M, Jain M, Dhawan DK. Modulatory effects of curcumin in conjunction with piperine on benzo(a)pyrene-mediated DNA adducts and biotransformation enzymes. Nutr Cancer. 2013;65:885–90. doi:10.1080/01635581.2013.805421.
32. Aadinath W, Bhushani A, Anandharamakrishnan C. Synergistic radical scavenging potency of curcumin-in-β-cyclodextrin-in-nanomagnetoliposomes. Mater Sci Eng C Elsevier BV. 2016;64:293–302.
33. Began G, Sudharshan E, Appu Rao AG. Inhibition of lipoxygenase 1 by phosphatidylcholine micelles-bound curcumin. Lipids. 1998;33:1223–8.
34. Belcaro G, Cesarone MR, Dugall M, Pellegrini L, Ledda A, Grossi MG, *et al*. Product-evaluation registry of Meriva®, a curcumin-phosphatidylcholine complex, for the complementary management of osteoarthritis. Panminerva Med. 2010;52:55–62.
35. Sehgal A, Kumar M, Jain M, Dhawan D. Piperine as an adjuvant increases the efficacy of curcumin in mitigating benzo(a)pyrene toxicity. Hum Exp Toxicol. 2012;31:473–82.
36. Hans ML, Lowman AM. Biodegradable nanoparticles for drug delivery and targeting. Curr Opin Solid State Mater Sci. 2002;6:319–27.
37. Cho K, Wang X, Nie S, Chen Z, Shin DM. Therapeutic nanoparticles for drug delivery in cancer. Clin Cancer Res. 2008;14:1310–6.
38. Yallapu MM, Gupta BK, Jaggi M, Chauhan SC. Fabrication of curcumin encapsulated PLGA nanoparticles for improved therapeutic effects in metastatic cancer cells. J Colloid Interface Sci. 2010;351:19–29. doi:10.1016/j.jcis.2010.05.022.
39. Kumar SSD, Mahesh A, Mahadevan S, Mandal AB. Synthesis and characterization of curcumin loaded polymer/lipid based nanoparticles and evaluation of their antitumor effects on MCF-7 cells. Biochim Biophys Acta Gen Subj. 1840;2014:1913–22. doi:10.1016/j.bbagen.2014.01.016.
40. Liu J, Xu L, Liu C, Zhang D, Wang S, Deng Z, *et al*. Preparation and characterization of cationic curcumin nanoparticles for improvement of cellular uptake. Carbohydr Polym. 2012;90:16–22.
41. Chuah LH, Billa N, Roberts CJ, Burley JC, Manickam S. Curcumin-containing chitosan nanoparticles as a potential mucoadhesive delivery system to the colon. Pharm Dev Technol. 2013;18:591–9. doi:10.3109/10837450.2011.640688.
42. Illum L. Chitosan and its use as a pharmaceutical excipient. Pharm Res. 1998;15:1326–31.
43. Stephen-Haynes J, Gibson E, Greenwood M. Chitosan: a natural solution for wound healing. J Community Nurs. 2014;28:48–53.
44. Dyer AM, Hinchcliffe M, Watts P, Castile J, Nankervis R, Smith A, *et al*. Nasal delivery of insulin using novel chitosan based formulations: a comparative study in two animal models between simple chitosan formulations and chitosan nanoparticles. Pharm Res. 2002;19:998–1008.
45. Malathi B, Mona S, Thiyagarajan D, Kaliraj P. Immunopotentiating nano-chitosan as potent vaccine carter for efficacious prophylaxis of filarial antigens. Int J Biol Macromol. 2015;73:131–7. doi:10.1016/j.ijbiomac.2014.11.014.
46. Berthold A, Cremer K, Kreuter J. Preparation and characterization of chitosan microspheres as drug carrier for prednisolone sodium phosphate as model for anti-inflammatory drugs. J Control Release. 1996;39:17–25.
47. Islam MA, Firdous J, Choi YJ, Yun CH, Cho CS. Design and application of chitosan microspheres as oral and nasal vaccine carriers: an updated review. Int J Nanomedicine. 2012;7:6077–93.
48. Maurstad G, Stokke BT, Vårum KM, Strand SP. PEGylated chitosan complexes DNA while improving polyplex colloidal stability and gene transfection efficiency. Carbohydr Polym. 2013;94:436–43. doi:10.1016/j.carbpol.2013.01.015.
49. Srivastava P, Malviya R. Sources of pectin, extraction and its applications in pharmaceutical industry—an overview. Indian J Nat Prod Resour. 2011;2:10–8.
50. Pérez Espitia PJ, Du WX, de Jesús Avena-Bustillos R, de Fátima Ferreira Soares N, McHugh T. Edible films from pectin: physical-mechanical and antimicrobial properties—a review. Food Hydrocoll. 2014;35:287–96. doi:10.1016/j.foodhyd.2013.06.005.
51. Liu L, Fishman ML, Hicks KB. Pectin in controlled drug delivery—a review. Cellulose. 2006;14:15–24.
52. He W, Du Q, Cao DY, Xiang B, Fan LF. Study on colon-specific pectin/ethylcellulose film-coated 5-fluorouracil pellets in rats. Int J Pharm. 2008;348:35–45.
53. Thirawong N, Nunthanid J, Puttipipatkhachorn S, Sriamornsak P. Mucoadhesive properties of various pectins on gastrointestinal mucosa: an in vitro evaluation using texture analyzer. Eur J Pharm Biopharm. 2007;67:132–40.
54. Syed Mohamad Al-Azi SO, Tan YTF, Wong TW. Transforming large molecular weight pectin and chitosan into oral protein drug nanoparticulate carrier. React Funct Polym. 2014;84:45–52. doi:10.1016/j.reactfunctpolym.2014.09.005.
55. Wichitnithad W, Jongaroonngamsang N, Pummangura S, Rojsitthisak P. A simple isocratic HPLC method for the simultaneous determination of curcuminoids in commercial turmeric extracts. Phytochem Anal. 2009;20:314–9.
56. Bhatta RS, Chandasana H, Chhonker YS, Rathi C, Kumar D, Mitra K, *et al*. Mucoadhesive nanoparticles for prolonged ocular delivery of natamycin: in vitro and pharmacokinetics studies. Int J Pharm. 2012;432:105–12. doi:10.1016/j.ijpharm.2012.04.060.
57. Takeuchi H, Thongborisute J, Matsui Y, Sugihara H, Yamamoto H, Kawashima Y. Novel mucoadhesion tests for polymers and polymer-coated particles to design optimal mucoadhesive drug delivery systems. Adv Drug Deliv Rev. 2005;57:1583–94.
58. Manolova Y, Deneva V, Antonov L, Drakalska E, Momekova D, Lambov N. The effect of the water on the curcumin tautomerism: a quantitative approach. Spectrochim Acta A Mol Biomol Spectrosc. 2014;132:815–20. doi:10.1016/j.saa.2014.05.096.
59. Li Z-Z, Wen L-X, Shao L, Chen J-F. Fabrication of porous hollow silica nanoparticles and their applications in drug release control. J Control Release. 2004;98:245–54.
60. Fan W, Yan W, Xu Z, Ni H. Formation mechanism of monodisperse, low molecular weight chitosan nanoparticles by ionic gelation technique. Colloids Surf B: Biointerfaces. 2012;90:21–7. doi:10.1016/j.colsurfb.2011.09.042.
61. Kolev TM, Velcheva EA, Stamboliyska BA, Spiteller M. DFT and experimental studies of the structure and vibrational spectra of curcumin. Int J Quantum Chem. 2005;102:1069–79.
62. Paulino AT, Simionato JI, Garcia JC, Nozaki J. Characterization of chitosan and chitin produced from silkworm crysalides. Carbohydr Polym. 2006;64:98–103.

63. Das RK, Kasoju N, Bora U. Encapsulation of curcumin in alginate-chitosan-pluronic composite nanoparticles for delivery to cancer cells. Nanomed Nanotechnol Biol Med. 2010;6:153–60. doi:10.1016/j.nano.2009.05.009.
64. Shi L, Gunasekaran S. Preparation of pectin-ZnO nanocomposite. Nanoscale Res Lett. 2008;3:491–5.
65. Gopi D, Kanimozhi K, Bhuvaneshwari N, Indira J, Kavitha L. Novel banana peel pectin mediated green route for the synthesis of hydroxyapatite nanoparticles and their spectral characterization. Spectrochim Acta A Mol Biomol Spectrosc. 2014;118:589–97. doi:10.1016/j.saa.2013.09.034.
66. Mi F-L, Sung H-W, Shyu S-S, Su C-C, Peng C-K. Synthesis and characterization of biodegradable TPP/genipin co-crosslinked chitosan gel beads. Polymer (Guildf). 2003;44:6521–30.
67. Martins AF, de Oliveira DM, Pereira AGB, Rubira AF, Muniz EC. Chitosan/TPP microparticles obtained by microemulsion method applied in controlled release of heparin. Int J Biol Macromol. 2012;51:1127–33. doi:10.1016/j.ijbiomac.2012.08.032.
68. Sarmento B, Ferreira D, Veiga F, Ribeiro A. Characterization of insulin-loaded alginate nanoparticles produced by ionotropic pre-gelation through DSC and FTIR studies. Carbohydr Polym. 2006;66:1–7.
69. Bansil R, Turner BS. Mucin structure, aggregation, physiological functions and biomedical applications. Curr Opin Colloid Interface Sci. 2006;11:164–70.
70. Kashyap D. Applications of pectinases in teh commercial sector: a review. Bioresour Technol Amsterdam. 2001;77:215–27.
71. Yu CY, Cao H, Zhang XC, Zhou FZ, Cheng SX, Zhang XZ, *et al*. Hybrid nanospheres and vesicles based on pectin as drug carriers. Langmuir. 2009;25:11720–6.
72. Munjeri O, Collett JH, Fell JT. Hydrogel beads based on amidated pectins for colon-specific drug delivery: the role of chitosan in modifying drug release. J Control Release. 1997;46:273–8.
73. Das S, Chaudhury A, Ng KY. Preparation and evaluation of zinc-pectin-chitosan composite particles for drug delivery to the colon: role of chitosan in modifying in vitro and in vivo drug release. Int J Pharm. 2011;406:11–20. doi:10.1016/j.ijpharm.2010.12.015.